# Carbonate dynamics and opportunities with low temperature, AEM-based electrochemical $CO_2$ separators

*William A. Rigdon,[a,b] Travis J. Omasta,[a,b] Connor Lewis,[a,b] Michael A. Hickner,[c] John R. Varcoe,[d] Julie N. Renner,[e] Kathy E. Ayers[e] and William E. Mustain[a,b,*]*

[a] Department of Chemical & Biomolecular Engineering, University of Connecticut, Storrs, CT.

[b] Center for Clean Energy Engineering, University of Connecticut, Storrs, CT.

[c] Department of Materials Science and Engineering, Pennsylvania State University, State College, PA.

[d] Department of Chemistry, University of Surrey, Guildford, UK.

[e] Proton OnSite, Wallingford, CT.

[*] Corresponding Author: mustain@engr.uconn.edu

KEYWORDS: carbon dioxide ($CO_2$), electrolysis, carbonate, bicarbonate, electrochemical separation (pump), anion exchange membrane (AEM)

## AUTHOR INFORMATION

### Corresponding Author

* email: mustain@engr.uconn.edu; phone: +1 860-486-2756; Address: 191 Auditorium Road, Unit 3222. Storrs, CT 06269-3222

## ABSTRACT

Fossil fuel power plants are responsible for a significant portion of anthropogenic atmospheric carbon dioxide ($CO_2$) and due to concerns over global climate change, finding solutions that significantly reduce emissions at their source has become a vital concern. When oxygen ($O_2$) is reduced along with $CO_2$ at the cathode of an anion exchange membrane (AEM) electrochemical cell, carbonate and bicarbonate are formed which are transported through electrolyte by migration from the cathode to the anode where they are oxidized back to $CO_2$ and $O_2$. This behavior makes AEM-based devices scientifically interesting $CO_2$ separation devices or "electrochemical $CO_2$ pumps." Electrochemical $CO_2$ separation is a promising alternative to state-of-the-art solvent-based methods because the cells operate at low temperatures and scale with surface area, not volume, suggesting that industrial electrochemical systems could be more compact than amine sorption technologies. In this work, we investigate the impact of the $CO_2$ separator cell potential on the $CO_2$ flux, carbonate transport mechanism and process costs. The applied electrical current and $CO_2$ flux showed a strong correlation that was both stable and reversible. The dominant anion transport pathway, carbonate vs. bicarbonate, undergoes a shift from carbonate to mixed carbonate/bicarbonate with increased potential. A preliminary techno-economic analysis shows that despite the limitations of present cells, there is a clear pathway to meet the US DOE 2025 and 2035 targets for power plant retrofit $CO_2$ capture systems through materials and systems-level advances.

## 1. INTRODUCTION

The threat of global climate change has brought considerable attention to the need for a reduction in anthropogenic $CO_2$ emissions. Captured $CO_2$ can be injected into existing geological formations or oil reservoirs, which can dramatically increase the productivity of previously depleted wells as well as allow the simultaneous, permanent, and safe storage of $CO_2$.[1,2] The U.S. Geological Survey recently reported that the U.S. alone has the potential for the storage of 3000 gigaton of $CO_2$ (~550 years emissions).[3] The $CO_2$ could also be used as an industrial solvent, or even reduced chemically or biologically to fuels,[4,5] potentially creating new economic opportunities and jobs.

The most significant sources for $CO_2$ emissions are electric power plants, accounting for around 35% of global emissions.[6,7] Unlike transportation emissions, a collection of millions of small sources of $CO_2$, there are only *ca.* 7300 electricity generation sites across the U.S., while more than 50% of emissions come from the largest 250 plants.[8] These relatively few high emission sites are prime targets for immediate action towards the reduction of $CO_2$ released into the Earth's atmosphere. As energy demands are steadily rising and supply is met through the combustion of fossil fuels, there is motivation to study methods that separate and concentrate $CO_2$ from power plant flue gas.

Chemical sorption is widely viewed as the state-of-the-art technology for scrubbing $CO_2$ from flue gas. A thermo-chemical amine (e.g. monoethanolamine) solvent-based absorption process is typically used for capture through chemical reduction. Recovery is achieved through thermal oxidation, releasing a concentrated $CO_2$ gas stream. There are two major disadvantages to using chemical sorption for $CO_2$ capture at larges scales: 1) The necessity for large amounts of sorbent material that scales with the amount of $CO_2$ captured, rapidly increasing the system size and cost

with scale-up. Theoretically, monoethanolamine requires two molecules for every $CO_2$ molecule removed.[9] Additionally, flue gas $CO_2$ is dilute (12-14%), introducing mass transport issues into the system. To compensate for this, some studies have shown that the amine:$CO_2$ ratio can be as high as 9;[10] and 2) The heating requirement to regenerate the amine.[11] A recent report projected that adding an amine sorption $CO_2$ system to a new pulverized coal power plant would increase the cost of electricity by 80% and de-rate the plant's net generating capacity by approximately 30%;[1] other studies show that the energy penalty may be as high as 45%.[6,10,12] Also, the steam temperature needed for efficient $CO_2$ desorption in the scrubber thermally degrades the amine over time to corrosive byproducts that cause vessel corrosion and additional costs are incurred because of the need to replace the capture solvent.

Though amine-based $CO_2$ capture processes have been in continuous development since the 1930's, and there are small power and industrial plants that have used this process to recycle $CO_2$ as a solvent,[12] the cost-benefit analysis is quite different for larger $CO_2$ capture and storage compared to these existing markets. The U.S. Department of Energy (DOE) has set a 2020-2025 capture target of \$45/tonne of $CO_2$ for retrofit coal-fired power plants and even more stringent cost targets for new plants.[1] Existing sorption systems have an average $CO_2$ capture cost of \$61/tonne of $CO_2$ (assuming a generation revenue loss of \$0.075 USD/kWh – the peak industrial rate in 2014[13] – and a capital cost amortization of 6 years with a \$6 USD/tonne of $CO_2$ operational cost[12]) and it will still be decades before the existing targets are met.[1] The excessive energy requirements and high cost of state-of-the-art amine-based $CO_2$ capture systems are the same reasons that sorption technology was considered unacceptable at the power plant scale 25 years ago.[14] Therefore, there is an urgent need for new technologies that approach $CO_2$ capture from

a fresh perspective in order to meet these challenging cost targets with a reasonable development time.

Electrochemical processes are promising alternatives for the separation, concentration, and compression of $CO_2$ since they are not bound by thermochemical cycles and so their theoretical energy requirements will always be lower [15–17] [REFS. High temperature electrochemical cells based on ceramic and molten carbonate electrolytes have been considered [18–21], but these systems require high heat input and suffer dynamic (operation) instabilities in addition to the electrical cost, making low temperature systems more suitable for large-scale $CO_2$ separation. One low temperature electrochemical approach that has been recently explored is the sorption of $CO_2$ by electrochemically reduced disulfides (thiolates) in tetraalkyl phosphonium/ammonium ionic liquid (IL) leading to the formation of thiocarbonates.[22–24] In a secondary step, the thiocarbonates are chemically transformed back to the disulfides and high purity $CO_2$ is released. This process has some very attractive features, including a mechanism naturally requiring only 1 electron per $CO_2$ molecule and there is also no need to generate steam for high quality heat; both act to reduce the energy required for $CO_2$ capture and highlight the technology's potential. However, there are a few potential drawbacks of this approach including: 1) likely high operating voltage; 2) low gas mass transport into IL; 3) low ionic conductivity for IL; and 4) cost and scalability of IL.

Low-temperature anion exchange membrane (AEM) electrochemical $CO_2$ separators are a relatively unexplored, yet promising, technology for low energy, low cost $CO_2$ separation from power plant flue gas. AEM-based $CO_2$ separators are in their infancy with limited previous work reported. The very earliest work utilized a porous membrane soaked in aqueous bicarbonate electrolyte with nickel mesh electrodes.[25–27] These devices were run at very high operating

voltages, which led to energy requirements for $CO_2$ separation that would be 200% of the generated power plant energy in some cases. Another serious problem with such high operating voltages is water electrolysis and unwanted corrosion reactions, resulting in low faradaic efficiencies. More recently, Kitchin *et al.* successfully operated an electrochemical $CO_2$ device with nickel catalysts at 1.2 V at room temperature.[28,29] Their device had a significantly improved energy footprint over previous electrochemical devices, requiring only 78% of the power plant output to separate $CO_2$ (approximately two times that of amine sorption) despite the fact that they used low surface area catalysts and lower performing anionic ionomer compared to the existing state-of-the-art. Additionally, their work focused primarily on the anode catalyst, with minimal consideration for the cathode catalyst, electrode structure, and electrolyte; probably the most important components which control the reaction selectivity and anion transport resistance of the cell. Additionally, their work did not capture the potential dependence of the reaction selectivity and $CO_2$ separation performance, and hence very little is currently known about the system dynamics. Therefore, several scientific and engineering questions remain and significant opportunities are available for rapid and transformational innovations in component and cell design, operation, system costs, and performance.

In this study, the potential voltage dependent dynamics of $CO_2$ separation are explored through coupled (simultaneous) current density and $CO_2$ effluent concentration measurements. Several important characteristics are assessed including: the operating current, the relationship between current and $CO_2$ exchange rate, cell reversibility and performance hysteresis, the dominant anion transport pathway, electrical cost, and the impact of operation on the thermodynamic efficiency of a typical coal fired power plant. We also report a preliminary techno-economic analysis that

explores both the energy and capital costs of the system to show the promise of AEM-based electrochemical separators to meet cost targets at the 500 MW power plant scale.

## 2. THEORY & OPERATION OF AEM-BASED $CO_2$ SEPARATORS

An illustration showing the operating principle of an AEM-based $CO_2$ separation cell is presented in Figure 1.

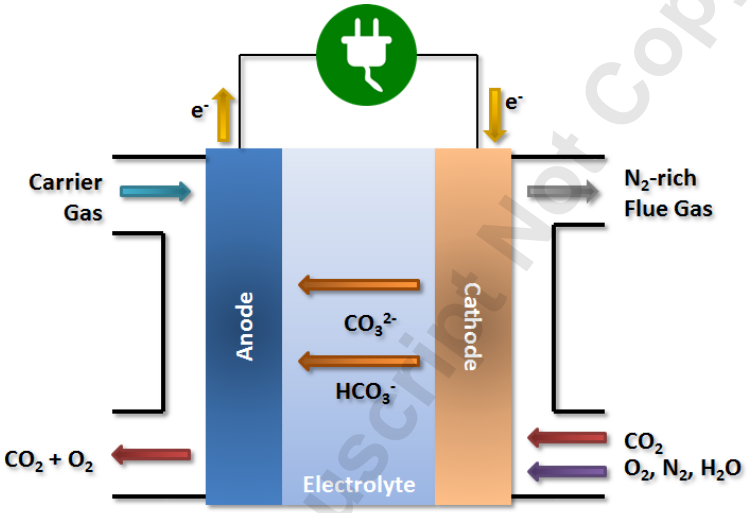


**Figure 1.** Operating principles of an AEM electrolyte electrochemical $CO_2$ separator.

The exhaust from a coal-fired or natural gas-fired power plant is fed to the cathode where the $CO_2$ and $O_2$ are separated from the incoming flue gas via electrocatalytic reduction to carbonate ($CO_3^{2-}$) and bicarbonate ($HCO_3^-$) anions. An indirect carbonate path requires $O_2$ reduction as a primary step (Equation 1) – the reaction then proceeds through non-electrochemical pathways initially yielding $HCO_3^-$ (Equation 2) followed by $CO_3^{2-}$ (Equation 3).

A direct carbonate path is also possible for $CO_3^{2-}$ generation (Equation 4), where bicarbonate can be subsequently produced via the reverse of the reaction presented in Equation 3.

149 $$O_2 + 2H_2O + 4\ e^- \rightarrow 4OH^- \quad (1)$$

150 $$2OH^- + 2CO_2 \rightarrow 2\ HCO_3^- \quad (2)$$

151 $$2OH^- + 2HCO_3^- \leftrightarrow 2CO_3^{2-} + 2H_2O \quad (3)$$

152 $$O_2 + 2CO_2 + 4\ e^- \rightarrow 2CO_3^{2-} \quad (4)$$

153 The $CO_3^{2-}/HCO_3^-$ anions are transported across an AEM to the anode where they are electrolyzed
154 back to $CO_2$ and $O_2$. The implications of Equations 1-4 are interesting, and critical to understanding
155 the operation of the device. No matter which reaction(s) dominate, four electrons are required per
156 mol of oxygen reduced. These electrons can be balanced by either carbonate or bicarbonate
157 transport through the electrolyte. If bicarbonate is the dominant anion, four $CO_2$ molecules are
158 transported through the membrane; another way to consider this is that only 1 electron is required
159 per separated $CO_2$ ($n$ = 1). If carbonate is the dominant anion, its divalence leads to only 2 $CO_2$
160 molecules being separated per reduced oxygen, or that 2 electrons are required per separated $CO_2$
161 ($n$ = 2). This has practical implications to these devices, which will be discussed further in Section
162 4.

163 In practical engineered systems, the anode carrier gas will be defined by the final application.
164 In the context of a power plant, the carrier gas for the $CO_2/O_2$ stream would most likely be methane,
165 which would be oxy-combusted to yield high purity $CO_2$ after condensing out the water.[28] Of
166 course, the oxy-combustor and condenser will add capital cost to the system, and the condenser
167 will require electricity to operate; however this can be offset by the energy produced through oxy-
168 combustion. It should also be noted that the water balance and management in the AEM-based
169 $CO_2$ separator will need to be considered in larger engineered system. Due to the relative infancy
170 of these devices, the costs and credits associated with the oxy-combustor, and condenser and
171 recycle will not be elaborated in this work. The carrier gas used here was high purity $N_2$.

Carbonates (and $CO_2$) have long been considered, and treated as, poisons in low temperature aqueous alkaline systems (*i.e.* alkaline fuel cells containing aqueous KOH electrolytes) due to the low solubility of alkali metal carbonate salts in free water. However, AEMs do not form these insoluble compounds because the carbonate anions are associated with stationary (already solid state) cationic groups fixed to the polymer backbone.[30] As a result, carbonate-based AEM systems have become an active research topic as interest in alkaline membrane electrochemistry and electrochemical devices has drastically increased in the last decade.[30–33] Some research has even targeted the specific utilization of carbonates through the study of new catalysts and understanding of fundamental anion transport/exchange mechanisms.[5,34–41] Use of a (bi)carbonate conducting polymer electrolyte cell has several important implications for commercial applications. Although the development of these cells needs to be advanced, improvements could result in a range of exciting new technologies. Separation of $CO_2$ from flue gas exhausted at power plants is just one promising possibility since capture and compression of $CO_2$ is valuable to many other applications. A low temperature, low cost anion conducting fuel cell that operates on air and resists carbonation can become a real possibility.[42] Furthermore, the conversion (partial oxidation) of hydrocarbon fuels to value added products in the anode of an electrochemical carbonate cell may be a further possibility.[39] Notably, $CO_2$ reduction and carbonate anion-exchange yield a large range of new opportunities at low (potentially near room) temperatures.

## 3. MATERIALS AND METHODS

An AEM-based $CO_2$ separator cell was assembled with commercial Pt cathode and anode catalysts, a poly(2,6-dimethyl-1,4-phenylene oxide) (PPO) quaternary ammonium (QA)

AEM[31], a radiation-grafted QA anion-exchange ionomer (AEI),[43] and operated at 50 ºC with no back pressure.

### 3.1 Electrode preparation

50 wt% platinum on Vulcan XC-72R (BASF) electrocatalysts were used at both the anode and cathode. AEI powders (ion exchange capacity, IEC, = 1.24 mmol $g^{-1}$) were prepared from radiation-grafted ETFE-powder and contained benzyltrimethylammonium functionality.[43] The AEI was hand-ground (milled) with a mortar and pestle for 10 min with dry electrocatalyst and the AEI comprised 15% of total catalyst layer mass. The solids were wetted with 2-3 mL DI water before suspension in 10 mL of isopropanol solvent using ultrasonic mixing for 30 min to form an electrode ink. Ink suspensions were spray deposited with an air brush onto Toray PTFE-treated carbon paper (TGP-H-030) to achieve a 0.5 $mg_{Pt}/cm^2$ loading; this was then cut into 5 $cm^2$ square gas diffusion electrodes (GDE).

### 3.2 Polymer anion exchange membrane

The synthesis as well as the physical and electrochemical characterization of the PPO membrane used in this work was extensively described previously [31]. Briefly, PPO with *ca.* 40% degree of bromination (40 % of the repeat units were brominated) was reacted with trimethylamine ($Me_3N$) and then cast into an AEM. The average thickness of the dry AEM was 57 ±3 μm and the IEC = 2.20 mmol $g^{-1}$ (calculated in the $Br^-$ form). Before cell construction, the AEM was soaked in aqueous $Na_2CO_3$ (1 M) for 2 h and then thoroughly rinsed in DI water (to remove the excess $Na_2CO_3$ species).

### 3.3 Cell construction and operation

A symmetric single cell was assembled using Fuel Cell Technologies (Albuquerque, NM) hardware with carbon graphite plates containing single serpentine flow channels and gold plated current collectors. Membrane electrode assemblies were fabricated in the cell hardware at room temperature by sandwiching the AEM between the GDE-supported anode and cathode electrodes. The GDEs were bordered with 127 μm thick Tefzel ETFE gaskets, resulting in *ca.* 30% compressive pinch. Once aligned, the cell was sealed using 7 N·m torque on the eight cell sealing bolts. A Scribner 850e test station controlled the temperature of the cell (50 °C) and the gas flows (100 % relative humidity, 0.2 standard L $min^{-1}$). The cathode gas supply was equivalent volumes of $CO_2$ and $O_2$ (with the exception of $O_2$-only control experiments), while high purity $N_2$ was supplied to the anode. It should be noted that tests were performed several times on multiple cells and the cell performance and behavior was highly repeatable. A representative data set from a single cell is presented.

### 3.4 Electrochemical cell tests

An Autolab PGSTAT302N was used to control the applied cell potential. Dynamic test were run using linear sweep voltammetry (LSV). LSVs were collected from 0.0 to +1.0 V at 5 mV $s^{-1}$ scan rate. A series of chronoamperometry (CA) steps were also performed from +0.1 V to +1.5 V and then back to +0.1 V with each step held for 30 min. Electrochemical impedance spectroscopy (EIS) experiments were used to determine the high frequency resistance (10 mV perturbations and frequency sweep from 50 → 0.5 kHz).

### 3.5 Carbon dioxide measurements

The $CO_2$ gas evolved from the anode was monitored continuously using a PP Systems SBA-5 gas analyzer and accompanying software, which utilizes a highly $CO_2$ selective non-dispersive infrared (NDIR) spectroscopy technique to measure the $CO_2$ concentration. The baseline $CO_2$ crossover in the cell was determined prior to each experiment and was subtracted from the raw data. The anode exhaust was first passed through an ice water chilled glass condensation bulb to prevent liquid from entering the detection chamber. The sweep gas flow rate was measured using an Agilent Digital Flowmeter Optiflow 650 and was used in estimating the molar evolution rates of $CO_2$. The high $N_2$ anode carrier gas flowrate (200 mL/min), was used in order to limit the $CO_2$ content of the anode < 1000 ppm in order to stay within the NDIR calibrated range and minimize response time. Therefore, the detected and reported $CO_2$ content of the anode is not a limiting value, it is purposefully, and artificially, low.

## 4. RESULTS & DISCUSSION

To verify that $CO_2$ was removed from the cathode feed due to the electrical stimulus and not diffusion, control experiments were initially performed. First, humidified $O_2$ was fed to the cathode and then, in a second experiment, the cathode was supplied with a feed containing an equivalent volume mixture of $O_2$ and $CO_2$. Both cells were polarized by LSV up to a cell potential of 1.0 V and coupled cell current/$CO_2$ anode emission measurements were recorded (Figure 2). Notably, the polarization curve showed a decrease in performance when operated with only $O_2$ and the $CO_2$ evolved at the anode was significantly less than the experiment with 50% $CO_2$. The amount of evolved $CO_2$ at the anode in the $O_2$-only cathode supply control experiment was non-zero and has several possible origins. One source may be de-carbonation of the AEM when the $OH^-$ anions

produced at the cathode displace $CO_3^{2-}/HCO_3^-$ anions persisting in the polymer electrolyte. However, carbon support and GDL material corrosion at higher anode potentials is also possible.[44,45] Next, the cell was allowed to rest at the open circuit voltage with the 50:50 $CO_2/O_2$ cathode supply and the $CO_2$ crossover was measured as $1.6 \times 10^{-9}$ mol $s^{-1}$. The amount of $CO_2$ that could be transported by electro-osmotic drag was overestimated with the assumption of a relatively high drag coefficient of 4 mol of $CO_2$-saturated $H_2O$ (Henry's Law) per $e^-$, which accounted for less than 2% of the value measured in the effluent at +1.0 V. Each of these secondary $CO_2$ transport mechanisms (diffusion and drag) were unable to account for the $CO_2$ observed in the anode effluent during cell testing. This confirms that the driving force for the $CO_2$ separation was the redox chemistry occurring at the electrodes.

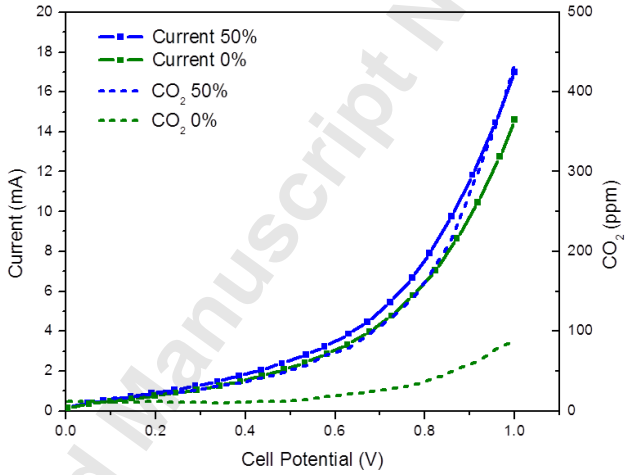


**Figure 2.** Comparison of applied current and $CO_2$ evolution at the anode with 0 %vol and 50 %vol $CO_2$ in the $O_2$-based cathode feed. The $N_2$ flowrate was set at 200mL/min to purposefully reduce the $CO_2$ concentration to < 1000 ppm.

Since the electrochemistry is the driving force for the $CO_2$ pumping action in this cell, it is important to understand how the cell potential impacts the electrochemical selectivity and effectiveness of the system. Steady-state observations showed a strong correlation between applied cell current and $CO_2$ evolution at the anode (Figure 3a). To measure the steady-state performance, a staircase was used where each 0.1 V step was held constant for 30 min while polarizing the cell

from +0.1 V → +1.5 V → +0.1 V. After each step change, the current and $CO_2$ crossover had sufficient time to stabilize, and the final data point from each step was taken to be the steady-state current. The data comparing the steady-state current and $CO_2$ evolution rate with respect to cell potential are presented in Figure 3b. Tests were performed several times and the cell performance and behavior was highly repeatable.

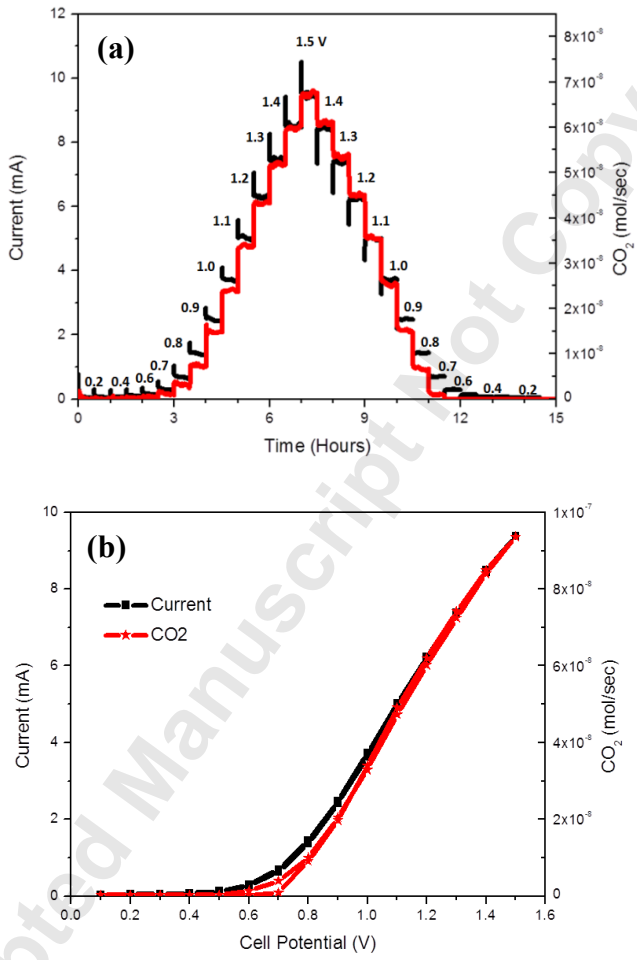


**Figure 3.** (a) Correlation of the applied cell current (black) and measured $CO_2$ evolution rate at the anode (red). (b) Current and $CO_2$ evolution rate *vs.* cell potential (forward and backward polarizations are shown).

The $CO_2$ evolution reversibly tracked the cell potential as shown in the overlapping anodic and cathodic polarization curves of Figure 3b, particularly at higher currents. There was minimal

hysteresis from the responsive system. The AEM and AEI used in this cell demonstrated good mechanical integrity and visual inspection of the membrane electrode assembly before and after testing suggested low dimensional swelling under full humidification. The high frequency area resistance (from EIS) was somewhat large in the representative data set, 55 Ω m, a value that needs further evaluation and improvement for a commercially-viable electrochemical reactor.

As the cell potential is increased, the cathode potential shifts negative and the relative driving forces for the reactions in Equations 1 – 4 change. The dynamic driving force with voltage means that the mechanism for anion formation and transport can change. The dominant anion transport ($CO_3^{2-}$ *vs.* $HCO_3^-$) mechanism was estimated from the number of electrons required to move each $CO_2$ molecule ($n$) from the feed stream (cathode) to the exhaust stream (anode). Equation 5 shows the relationship between $n$ and the cell operating current ($i$), Faraday's constant ($F$), the concentration of $CO_2$ in the anode stream in ppm ($C_{CO2}$) and the molar flowrate of the sweep gas in mol $s^{-1}$ ($M_G$) .

$$n = \frac{10^6 * i}{F * C_{CO2} * M_G} \quad (5)$$

The voltage dependence for the number of $e^-$ required to transport each $CO_2$ molecule is plotted in Figure 4. At very low currents (cell potential < 0.7 V), the amount of $CO_2$ measured at the anode was close to the NDIR detection limit, and $n$ was highly sensitive to slight variations in signal, leading to an artificial increase in $n$. Therefore, only data collected at cell potentials > 0.7 V were used to elucidate the potential dependence of the $CO_3^{2-}/HCO_3^-$ mechanism (represented in Figure 4). At 0.7 V, $n$ was slightly above 2, affirming $CO_3^{2-}$ conduction as the dominant anion transport pathway at low cell potentials. As the cell potential increased, there was a clear transition from $CO_3^{2-}$ to a near equal balance of $CO_3^{2-}/HCO_3^-$, where $n$ stabilized around a value of 1.5.

Journal of Electrochemical Energy Conversion and Storage. Received February 10, 2016;
Accepted manuscript posted April 20, 2016. doi:10.1115/1.4033411


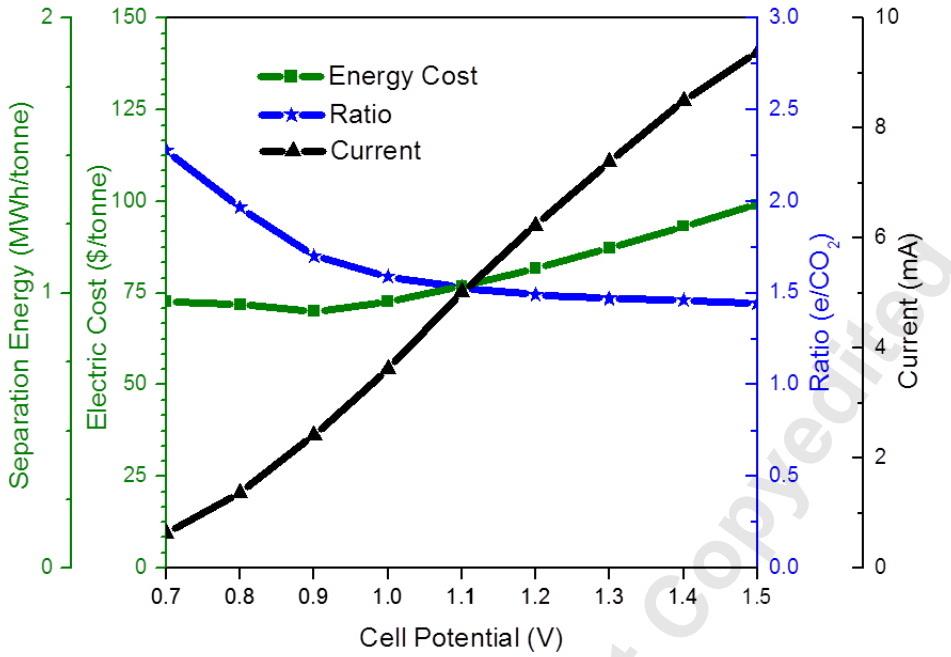


**Figure 4.** The number of electrons (blue) required to separate each $CO_2$ molecule coupled with the separation energy and electrical costs (green) as a function of the cell potential.

### 4.1 Energy requirements

The typical output of a coal-fired power plant normalized to its $CO_2$ emissions is approximately 1.1 MWh per tonne of $CO_2$. In AEM-based $CO_2$ separators, the energy requirement ($E_S$) for separation is controlled primarily by the cell potential ($V$) and $n$ as defined by Equation 6.

$$E_S\left(\frac{MWh}{tonne_{CO2}}\right) = \frac{nF|V|}{44.01*3600} \quad (6)$$

Therefore, the anode and cathode catalysts need to have low activation overpotentials, and the AEM must have high anion conductivity to minimize the cell potential. In addition, the cathode catalyst must provide the appropriate reaction selectivity, since the amount of energy required doubles when $CO_3^{2-}$ (n = 2) vs. $HCO_3^-$ (n = 1) production is favored at the same cell potential. On the practical size, $HCO_3^-$ is preferred mechanistically because of its much lower energy cost; however, bicarbonate operation does have one very important tradeoff: $HCO_3^-$ has a lower intrinsic

mobility than $CO_3^{2-}$ due to its larger hydration radius, which will lead to higher electrolyte (AEM) ionic resistivity thus higher cell voltage. The PPO membrane in this work was selected because of its high carbonate conductivity, relatively low water uptake and good mechanical strength [31]. However, chemical and mechanical durability are not the most important factors when choosing an AEM for this application since AEMs are intrinsically more stable in carbonate form than hydroxide form [30,46].

One distinct advantage of AEM-based $CO_2$ separation *vs.* chemical sorption is that the thermodynamic minimum energy requirement for $CO_2$ separation is 80% lower since electrochemical systems are not bound by thermochemical cycles. The minimum energy requirement for chemical sorption is approximately 11% of the power plant rating (~ 0.12 MWh per tonne $CO_2$) based on the heating requirement to produce steam and release $CO_2$ from the amine sorbent.[12] In contrast, the minimum for the AEM separator studied in this work is only 0.029 MWh per tonne $CO_2$ based on the Nernst equation (Equation 7), which is 2.6% of the power plant rating if the device is operated at 50 ºC (assuming an exclusive bicarbonate pathway).

$$V_T = \frac{RT}{nF} ln\left(\frac{P_{CO2,sep}}{P_{CO2,fluegas}}\right) \quad (7)$$

where $V_T$ is the thermodynamic cell voltage, $R$ is the ideal gas constant, $T$ is the temperature (K), $P_{CO2,sep}$ is the partial pressure of $CO_2$ in the anode exhaust, and $P_{CO2,fluegas}$ is the partial pressure of $CO_2$ in the cathode feed. Therefore, electrochemical AEM-based $CO_2$ separators have the potential for energy requirements that are not only less than the state-of-the-art, but are impossible to achieve with amine sorption.

The electrochemical operating space for a $CO_2$ separator is shown in Figure 5a. Operating at or above the power plant generation energy (1.1 MWh per tonne $CO_2$) is represented by the red region in Figure 5a. The span of energy requirements for existing chemical sorption technologies are

356 shown in orange. To date, investigators have not been able to achieve energy requirements that
357 approach the thermodynamic limit for electrochemical-based $CO_2$ separation, though this is to be
358 expected given the limited state of development of the technology; however, significant progress
359 has been made.

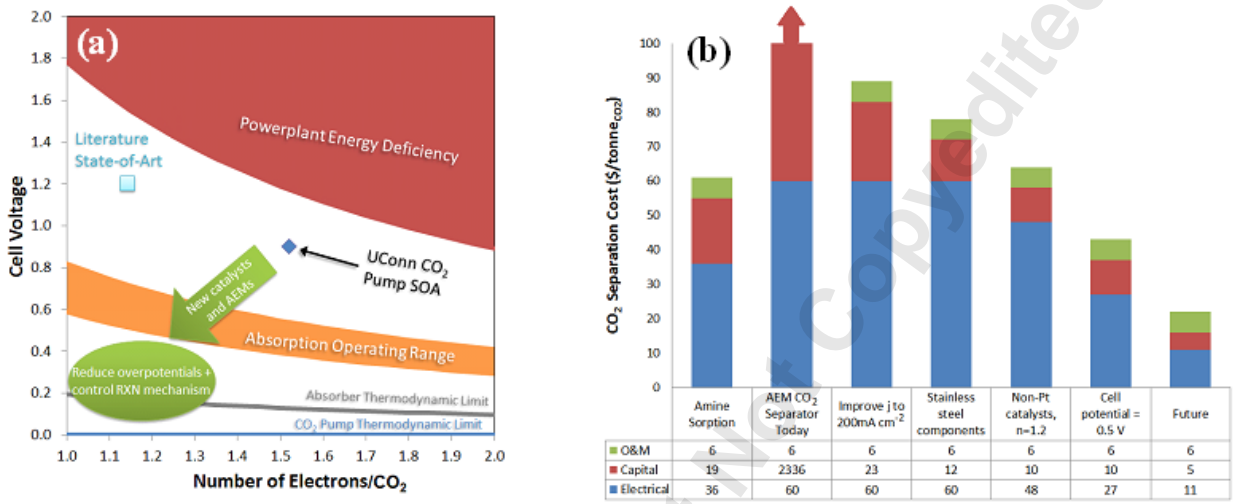


360

361 **Figure 5.** (a) Existing operating requirements for amine and electrochemical separation showing
362 how AEM-based electrochemical cell improvements can yield energy requirements below the
363 thermodynamic limit for chemical sorption; (b) influence of cell and stack improvements on the
364 cost of electrochemical $CO_2$ separation, showing that AEM-based electrochemical cell
365 improvements can lead to very low costs (*ca.* ⅓ of chemical amine sorption).

366

367 The first AEM cells operated around 2.5 V, which is an energy requirement of 1.57 MWh per
368 tonne $CO_2$ if $n$ = 1 (exclusive $HCO_3^-$ pathway) or 3.14 MWh per tonne $CO_2$ if $n$ = 2 (exclusive
369 $CO_3^{2-}$ pathway); these represent 140 and 280% of the power plant energy to operate, respectively,
370 which are obviously far too high for practical application.[25–27] Landon and Kitchin were able
371 to reduce the energy requirement to 0.88 MWh per tonne $CO_2$ (~78% power plant output) by
372 reducing the operating voltage to 1.2 V operating mostly on the $HCO_3^-$ cycle (light blue square in
373 Figure 5a).[29] Using Equation 5, the energy requirement for $CO_2$ separation was calculated for
374 the staircase experiments as a function of the cell potential (Figure 4). For this representative data

set, the lowest energy requirement was 0.93 MWh per tonne $CO_2$; however, our best performing cell had a lower $n$ = 1.47 at a cell potential of 0.9 V, yielding a $CO_2$ separations energy of 0.80 MWh per tonne $CO_2$ (72% of power plant output). Though this number will need to be improved, it represents the lowest energy requirement reported in the literature to date (dark blue diamond in Figure 5a).

In order to achieve AEM-based cells that approach the thermodynamic limit, researchers must not only make material advances to improve the cathode selectivity for bicarbonate, but also reduce the electrode overpotentials and membrane resistance. They should eliminate gaps in the scientific and operational knowledge by understanding the voltage dependence of the $CO_2$ separation dynamics, the relationship between current and $CO_2$ exchange rate, cell reversibility and stability, as well as the anion transport and redox mechanisms. These were all explored in this work; however, there is considerably more work that needs to be done to determine the influence of temperature, gas composition, impurities (i.e. $NH_3$, $H_2S$ are well known Pt poisons that are present in flue gas), as well as cell construction and operation variables on its performance. These will be the focus of our future work.

### 4.2 Preliminary Unit Operations Considerations and Cost

There are three primary cost drivers from a unit perspective: lost electrical generation, capital investment and amortization, and plant operation and maintenance (O&M). In amine scrubbing systems, the lost electrical generation cost stems from thermal de-rating of the power plant, while in the AEM-based system, electricity is internally rerouted and cannot be sold. Equation 8 calculates the electrical cost per tonne of $CO_2$ emitted from the power plant (results plotted in Figure 4).

$$\frac{\$}{tonne_{CO2}} = 1000 * E_S * \$0.075/kWh \quad (8)$$

For the representative data set in Figure 4, where the lowest energy requirement was 0.93 MWh per tonne of $CO_2$, the lost electrical generation cost would be \$70 per tonne of $CO_2$; however, the cell with the lowest measured $e^-/CO_2$ ratio of $n$ = 1.47 (at 0.9 V) would have an electrical cost of only \$60 per tonne of $CO_2$. Though this number is reasonably close to the cost target for the U.S. DOE 2025 target for a retrofit coal-fired power plant, it is only part of the picture since the capital and O&M costs must also be considered.

From a capital costs perspective, the primary drivers are the system materials (what is used for the cell hardware, catalysts, membranes and other components) and the operating current density. The flow of $CO_2$ out of a large coal-fired powerplant is very large; *e.g.* the rate from a typical 500 MW coal-fired power plant is more than 7.5 tonne $min^{-1}$. In order to operate at this scale, thousands of parallel $CO_2$ separator stacks would be needed to achieve complete separation and the number scales almost linearly with the operating current density. Based on the proprietary costs and estimates for existing Proton OnSite commercial stacks with their standard materials for the flow fields and cell separators, a 2 mA $cm^{-2}$ operating current (consistent with Figures 3 and 4), and the same catalysts and AEM/AEI used in this work, and amortizing the capital cost over 6 years, it was estimated that the existing $CO_2$ pump capital cost would be approximately \$2300 per tonne of $CO_2$. This is currently a very large cost, but not unexpected for an immature technology; this highlights the need to improve the cell performance and lower the cost of the materials of construction, which will be discussed in detail below.

Contributing to the excessive cost are three materials and systems-level properties that must all be improved in order to exceed the U.S. DOE 2025 cost targets:

1) Operating current density, which dictates the total system size and right now is the primary driver of the capital cost, should be increased from 2 mA $cm^{-2}$ to at least 200 mA $cm^{-2}$ by improving catalyst and AEM chemistry and structure, as well as improved electrode engineering. We can foresee the possibility since similar approaches have raised the operating current density of $OH^-$-based AEM systems from < 100 to > 1000 mA $cm^{-2}$ in the past five years, while simultaneously reducing the cell overpotentials.[30] One important consideration is that high current devices may have a higher portion of ions transporting through the system in $OH^-$ form, which would, in effect, reduce the faradaic efficiency of the device. Next-generation cells must maintain efficiencies, which can be achievable through carbonate-selective catalysts or membranes with high $CO_2$ permeability.

2) Replacing high cost materials, including titanium cell components with stainless steel, and platinum catalysts with non-noble metal catalysts[47] is facilitated in this concept because of the low corrosion $CO_3^{2-}/HCO_3^-$ (mildly alkaline) environments.

3) Reducing the cell operating voltage below 0.5 V (about 5 × the voltage required for existing $H_2$ pumping cells operating at 200 mA $cm^{-2}$) through innovations in the catalyst, AEM and AEI, while simultaneously reducing the $e^-/CO_2$ ratio below $n = 1.2$. Possible metrics include reduction of the cathode overpotential to < 0.3 V, anode overpotential < 0.2 V, and the combined AEM and contact overpotential < 0.025 V.

The projected cost reduction of an AEM-based electrochemical $CO_2$ separator with many of the innovations discussed above is shown in Figure 5b. For all cases, a constant $6 per tonne $CO_2$ O&M cost was assumed, which is consistent with sorption technology. Increasing the cell current density from the existing 2 mA $cm^{-2}$ to 200 mA $cm^{-2}$ reduces the capital cost to a reasonable value of $23 per tonne $CO_2$, on par with the capital cost for a typical amine sorption system. It should

443 also be noted that increasing the AEM separator current density to 200 mA $cm^{-2}$ yields a system
444 size of approximately 750 $m^3$, which is around ½ of the volume of the absorber/stripper/boiler that
445 it would replace from the chemical sorption system. Further cost savings by transitioning to
446 stainless steel stack components reduces the capital cost to around $12 per tonne $CO_2$.
447 Transitioning from Pt catalysts with moderate $HCO_3^-$ selectivity to high selectivity ($n$ = 1.2), non
448 Pt catalysts would reduce the capital cost further to $10 per tonne $CO_2$ and simultaneously reduce
449 the electrical cost from $60/ per tonne $CO_2$ to $48 per tonne $CO_2$. Lowering the operating voltage
450 to 0.5 V reduces the electrical cost to $27 per tonne $CO_2$.

451 When combined, these achievable innovations, which should be the R&D goals in the short
452 term, lead to a total cost for an AEM-based $CO_2$ separations system of $43 per tonne $CO_2$ – lower
453 than the U.S. DOE 2025 capture target of $45 per tonne $CO_2$ for retrofit coal-fired power plants.
454 Future, long-term, innovations can be expected to further reduce the operating voltage to 0.25 V
455 (still more than 2× the value for $H_2$ pumping), increase the $HCO_3^-$ selectivity to yield $n$ = 1 ($e^-$ per
456 $CO_2$ molecule) and increase the operating current to 1 A $cm^{-2}$ (consistent with the operating current
457 densities of state-of-the-art AEM-based fuel cells and electrolyzers). These innovations would
458 reduce the cost to around $22 per tonne $CO_2$, which is even lower than the U.S. DOE 2035 cost
459 target for retrofit plants ($30 per tonne $CO_2$).[1] Clearly, electrochemical $CO_2$ pumping has a long
460 way to go in its development. In addition to materials advances an important consideration for
461 future study is the possible impact of common flue gas impurities at relevant concentrations on the
462 operating current density, reaction mechanism and capture efficiency, i.e. CO (20 ppm),
463 hydrocarbons (10 ppm), HCl (100 ppm), $SO_2$ (800 ppm), and $NO_x$ (800 ppm). Also, the oxy-
464 combustion and water management scheme must be considered, designed and analysed. However,
465 the calculations and experiments in this work highlight the exciting ultimate potential for AEM-

based electrochemical $CO_2$ separators as a low energy, low cost option for $CO_2$ separation from flue gas in the near future.

## 5. CONCLUSIONS

An AEM-based electrochemical $CO_2$ separator was investigated and its future performance and cost metrics discussed. In these devices, (bi)carbonate anions are produced through the electrochemical reduction of $O_2 + CO_2$. The anions are transported from the cathode to the anode through an anion-exchange membrane (AEM) where they are electrolyzed back to $CO_2$ and $O_2$. In this work, the relationships between the cell potential and carbonate/bicarbonate selectivity were explored, giving valuable insight to reactions occurring while offering a roadmap for future investigations into improved cell design and construction materials. The cell current and $CO_2$ separation through the AEM were closely correlated. Carbonate and bicarbonate both played a role in anion exchange and transport through the cell, particularly at higher voltages. It was also found that the energy required, electrical cost and capital cost offer a positive perspective on the possible application of AEM-based electrochemical pumping technology for use in $CO_2$ separation. The AEM system reduces the thermodynamic barrier for $CO_2$ separation by 80% compared to conventional amine sorption process and there is a clear pathway to achieve systems costs that meet U.S. DOE 2025 and 2035 targets for retrofit coal-fired power plants. Therefore, AEM-based electrochemical $CO_2$ separation systems are a promising area for future research with the potential to have a high impact on the carbon capture and utilization landscape in the near future.



## ACKNOWLEDGMENT

The cell assembly and performance work in Professor Mustain's lab was supported by the U.S. DOE Early Career Program through Award Number DE-SC0010531. Professor Hickner

488 acknowledges partial support of this work by the United States-Israel Binational Science
489 Foundation (BSF) through Energy Project No. 2011521 and the backing of industrial sponsors.
490 The anion-exchange ionomer powders were synthesized using funds from Professor Varcoe's
491 EPSRC Fellowship (Grant EP/1004882/1): the raw IEC data for the AEI powders is available
492 without restriction [details at the University of Surrey publications repository at DOI:
493 dx.doi.org/10.15126/surreydata.00807830 (http://epubs.surrey.ac.uk/807830/).

## 494 ABBREVIATIONS

495 AEI, anion exchange ionomer; AEM, Anion Exchange Membrane; CA, chronoamperometry; EIS,
496 electrochemical impedance spectroscopy; ILs, Ionic Liquids; LSV, linear sweep voltammetry;
497 NDIR, non-dispersive infrared; PPO, poly-phenylene oxide; QA, quaternary ammonium;

## 498 REFERENCES

499 [1] 2013, Carbon Capture Technology Program Plan.
500 [2] Boot-Handford, M. E., Abanades, J. C., Anthony, E. J., Blunt, M. J., Brandani, S., Mac
501 Dowell, N., Fernández, J. R., Ferrari, M.-C., Gross, R., Hallett, J. P., Haszeldine, R. S.,
502 Heptonstall, P., Lyngfelt, A., Makuch, Z., Mangano, E., Porter, R. T. J., Pourkashanian, M.,
503 Rochelle, G. T., Shah, N., Yao, J. G., and Fennell, P. S., 2014, "Carbon capture and storage
504 update," Energy Environ. Sci., **7**, p. 130.
505 [3] 2013, National Assessment of Geologic Carbon Dioxide Storage Resources — Results.
506 [4] Dimitriou, I., García-Gutiérrez, P., Elder, R. H., Cuellar-Franca, R., Azapagic, A., and
507 Allen, R. W. K., 2015, "Carbon dioxide utilisation for production of transport fuels: process
508 and economic analysis," Energy Environ. Sci., **8**, pp. 1775–1789.
509 [5] Spinner, N. S., Vega, J. A., and Mustain, W. E., 2012, "Recent progress in the
510 electrochemical conversion and utilization of CO2," Catal. Sci. Technol., **2**(1), p. 19.

[6] Fisher, K. S., Street, S. A., Rochelle, G., and Figueroa, J. D., 2005, "Integrating MEA regeneration with CO2 compression to reduce CO2 capture costs," 4th Annual Conference on Carbon Capture and Sequestration DOE/NETL, pp. 1–11.

[7] U.S. Environmental Protection Agency, 2015, "Greenhouse Gas Emissions" [Online]. Available: http://www.epa.gov/climatechange/ghgemissions/.

[8] U.S. Energy Information Administration, 2013, "Independent Statistics and Analysis, Electricity" [Online]. Available: http://www.eia.gov/countries/analysisbriefs/Nigeria/nigeria.pdf.

[9] Yu, C., Huang, C., and Tan, C., 2012, "A Review of CO 2 Capture by Absorption and Adsorption," Aerosol Air Qual. Res., **12**, pp. 745–769.

[10] Zhai, R., and Yang, Y., 2010, "MEA-Based CO2 Capture Technology and Its Application in Power Plants," Paths to Sustainable Energy, J. Nathwani, and A. Ng, eds., InTech, pp. 499–511.

[11] Ho, M. T., Allinson, G. W., and Wiley, D. E., 2008, "Reducing the Cost of CO2 Capture from Flue Gases Using Pressure Swing Adsorption," Ind. Eng. Chem. Res., **47**, pp. 4883–4890.

[12] Rochelle, G. T., 2009, "Amine scrubbing for CO2 capture.," Science, **325**(5948), pp. 1652–1654.

[13] U.S. Energy Information Administration, 2015, "Independent Statistics & Analysis, Electricity, Sales (consumption), revenue, prices & customers" [Online]. Available: http://www.eia.gov/electricity/data.cfm#sales.

[14] Booras, G. S., and Smelser, S. C., 1991, "An engineering and economic evaluation of CO2 removal from fossil-fuel-fired power plants," Energy, **16**(11-12), pp. 1295–1305.

534 [15] White, C. M., Strazisar, B. R., Granite, E. J., Hoffman, J. S., and Pennline, H. W., 2003,
535 "Separation and capture of CO2 from large stationary sources and sequestration in
536 geological formations- coalbeds and deep saline aquifers," J. Air Waste Manage. Assoc.,
537 **53**(6), pp. 645–715.
538 [16] Granite, E. J., and O'Brien, T., 2005, "Review of novel methods for carbon dioxide
539 separation from flue and fuel gases," Fuel Process. Technol., **86**(14), pp. 1423–1434.
540 [17] Aaron, D., and Tsouris, C., 2005, "Separation of CO2 from flue gas: a review," Sep. Sci.
541 Technol., **40**(1-3), pp. 321–348.
542 [18] Manzolini, G., Campanari, S., Chiesa, P., Giannotti, A., Bedont, P., and Parodi, F., 2012,
543 "CO2 Separation From Combined Cycles Using Molten Carbonate Fuel Cells," J. Fuel Cell
544 Sci. Technol., **9**, p. 011018.
545 [19] Amorelli, A., Wilkinson, M. B., Bedont, P., Capobianco, P., Marcenaro, B., Parodi, F., and
546 Torazza, A., 2002, "An experimental investigation into the use of molten carbonate fuel
547 cells to capture CO2 from gas turbine exhaust gases," Energy, **29**, pp. 1279–1284.
548 [20] Winnick, J., Toghiani, H., and Quattrone, P. D., 1982, "Carbon dioxide concentration for
549 manned spacecraft using a molten carbonate electrochemical cell," AIChE J., **28**(1), pp.
550 103–111.
551 [21] Sugiura, K., Yanagida, M., Tanimoto, K., and Kojima, T., 2000, "The removal
552 characteristics of carbon dioxide in molten carbonate for the thermal power plant," Proc.
553 GHGT-5, Aust.
554 [22] Rheinhardt, J., and Buttry, D. A., 2014, "Energy Efficient Capture and Release of Carbon
555 Dioxide in Tetraalkyl Phosphonium and Tetraalkyl Ammonium Ionic Liquids," Meet.
556 Abstr., **MA2014-02**(25), p. 1431.

557 [23] Hasani, M., and Buttry, D., 2013, "Chemical Reactivity of Alkyl Thiolates Used in
558 Electrochemical CO2 Capture in Ionic Liquids," 224th ECS Meeting, p. 2601.
559 [24] Buttry, D. A., 2014, "Capture and Release of Carbon Dioxide."
560 [25] Li, K., and Li, N., 1993, "Removal of carbon dioxide from breathing gas mixtures using an
561 electrochemical membrane cell," Sep. Sci. Technol., **28**, pp. 1085–1090.
562 [26] Li, K., Teo, W., and Hughes, R., 1994, "Use of membranes for carbon dioxide removal in
563 underwater life support systems," Underw. Technol., **20**(1), pp. 13–17.
564 [27] Xiao, S., and Li, K., 1997, "On the use of an electrochemical membrane module for removal
565 of CO2 from a breathing gas mixture," Chem. Eng. Res. Des., **75**(4), pp. 438–446.
566 [28] Pennline, H. W., Granite, E. J., Luebke, D. R., Kitchin, J. R., Landon, J., and Weiland, L.
567 M., 2010, "Separation of CO2 from flue gas using electrochemical cells," Fuel, **89**(6), pp.
568 1307–1314.
569 [29] Landon, J., and Kitchin, J. R., 2010, "Electrochemical Concentration of Carbon Dioxide
570 from an Oxygen/Carbon Dioxide Containing Gas Stream," J. Electrochem. Soc., **157**(8), p.
571 B1149.
572 [30] Varcoe, J. R., Atanassov, P., Dekel, D. R., Herring, A. M., Hickner, M. A., Kohl, P. A.,
573 Kucernak, A. R., Mustain, W. E., Nijmeijer, K., Scott, K., Xu, T., and Zhuang, L., 2014,
574 "Anion-exchange membranes in electrochemical energy systems," Energy Environ. Sci.,
575 **7**(10), pp. 3135–3191.
576 [31] Li, N., Leng, Y., Hickner, M. A., and Wang, C. Y., 2013, "Highly stable, anion conductive,
577 comb-shaped copolymers for alkaline fuel cells," J. Am. Chem. Soc., **135**(27), pp. 10124–
578 10133.
579 [32] Hickner, M. A., Herring, A. M., and Coughlin, E. B., 2013, "Anion exchange membranes:

Current status and moving forward," J. Polym. Sci. Part B Polym. Phys., **51**(24), pp. 1727–1735.

[33] Grew, K. N., Ren, X., and Chu, D., 2011, "Effects of Temperature and Carbon Dioxide on Anion Exchange Membrane Conductivity," Electrochem. Solid-State Lett., **14**(12), p. B127.

[34] Kiss, A. M., Myles, T. D., Grew, K. N., Peracchio, A. A., Nelson, G. J., and Chiu, W. K. S., 2013, "Carbonate and Bicarbonate Ion Transport in Alkaline Anion Exchange Membranes," J. Electrochem. Soc., **160**(9), pp. F994–F999.

[35] Myles, T. D., Kiss, A. M., Grew, K. N., Peracchio, A. A., Nelson, G. J., and Chiu, W. K. S., 2011, "Calculation of Water Diffusion Coefficients in an Anion Exchange Membrane Using a Water Permeation Technique," J. Electrochem. Soc., **158**(7), p. B790.

[36] Vega, J. A., Shrestha, S., Ignatowich, M., and Mustain, W. E., 2012, "Carbonate Selective Ca2Ru2O7-y Pyrochlore Enabling Room Temperature Carbonate Fuel Cells," J. Electrochem. Soc., **159**(1), p. B12.

[37] Vega, J. A., Spinner, N., Catanese, M., and Mustain, W. E., 2012, "Carbonate Selective Ca2Ru2O7−y Pyrochlore Enabling Room Temperature Carbonate Fuel Cells," J. Electrochem. Soc., **159**(1), p. B19.

[38] Hancock, C. A., Ong, A. L., and Varcoe, J. R., 2014, "Effect of carbonate anions on Bi-doped Ca2Ru2O7 pyrochlores that are potential cathode catalysts for low temperature carbonate fuel cells," RSC Adv., **4**(57), p. 30035.

[39] Spinner, N., and Mustain, W. E., 2013, "Electrochemical Methane Activation and Conversion to Oxygenates at Room Temperature," J. Electrochem. Soc., **160**(11), pp. F1275–F1281.

[40] Spinner, N., and Mustain, W. E., 2011, "Effect of nickel oxide synthesis conditions on its

physical properties and electrocatalytic oxidation of methanol," Electrochim. Acta, **56**(16), pp. 5656–5666.

[41] Gunasekara, I., Lee, M., Abbott, D., and Mukerjee, S., 2012, "Mass Transport and Oxygen Reduction Kinetics at an Anion Exchange Membrane Interface: Microelectrode Studies on Effect of Carbonate Exchange," ECS Electrochem. Lett., **1**(2), pp. F16–F19.

[42] Li, G., Wang, Y., Pan, J., Han, J., Liu, Q., Li, X., Li, P., Chen, C., Xiao, L., Lu, J., and Zhuang, L., 2015, "Carbonation effects on the performance of alkaline polymer electrolyte fuel cells," Int. J. Hydrogen Energy, **40**(20), pp. 6655–6660.

[43] Poynton, S. D., Slade, R. C. T., Omasta, T. J., Mustain, W. E., Escudero-Cid, R., Ocón, P., and Varcoe, J. R., 2014, "Preparation of radiation-grafted powders for use as anion exchange ionomers in alkaline polymer electrolyte fuel cells," J. Mater. Chem. A, **2**, p. 5124.

[44] Roen, L. M., Paik, C. H., and Jarvi, T. D., 2004, "Electrocatalytic Corrosion of Carbon Support in PEMFC Cathodes," Electrochem. Solid-State Lett., **7**(1), p. A19.

[45] Shrestha, S., Liu, Y., and Mustain, W. E., 2011, "Electrocatalytic Activity and Stability of Pt clusters on State-of-the-Art Supports: A Review," Catal. Rev., **53**(3), pp. 256–336.

[46] Vega, J. A., Chartier, C., and Mustain, W. E., 2010, "Effect of hydroxide and carbonate alkaline media on anion exchange membranes," J. Power Sources, **195**(21), pp. 7176–7180.

[47] Wu, J., Yadav, R. M., Liu, M., Sharma, P. P., Tiwary, C. S., Ma, L., Zou, X., Zhou, X., Yakobson, B. I., Lou, J., and Ajayan, P. M., 2015, "Achieving Highly Efficient, Selective, and Stable CO2 Reduction on Nitrogen-Doped Carbon Nanotubes," Nano, **9**(5), pp. 5364–5371.